

Path Toward High-Efficiency CZTS Solar Cells with Buffer Layer Optimization

W. HENNI^{a,*}, W.L. RAHAL^{b,c} AND D. RACHED^d

^a*Elaboration and Characterization Physico-Mechanical and Metallurgical of Materials Laboratory, University Abdelhamid Ibn Badis of Mostaganem, Route National N° 11, Kharouba, 27000, Mostaganem, Algeria*

^b*Laboratory of Analysis and Application of Radiation, Faculty of Physics, University of Sciences and Technology of Oran Mohamed Boudiaf, BP 1505, el Mnaouar, Oran, Algeria*

^c*Physics Department, University Abdelhamid Ibn Badis of Mostaganem, Chemin des Crêtes, 27000, Mostaganem, Algeria*

^d*Laboratory of Plasma Physics, Conductive Materials and their Applications, University of Science and Technology of Oran Mohamed Boudiaf, BP 1505, el Mnaouar, Oran, Algeria*

Received: 03.01.2022 & Accepted: 07.09.2022

Doi: [10.12693/APhysPolA.142.445](https://doi.org/10.12693/APhysPolA.142.445)

*e-mail: wafaa.henni@gmail.com

In this work, we numerically improve the performance of kesterite thin film solar cells ($\text{ZnO}/\text{Cu}_2\text{ZnSnS}_4/\text{CdS}/\text{MoS}_2$) using the Solar Cell Capacitance Simulator. The work carried out is mainly based on the study of the influence of the doping density, the thickness, and the gap energy of the buffer layer on the cell's performance. Based on the simulation results, it is found that increasing the buffer layer thickness strongly deteriorates the cell's performance. An optimized and economical CdS buffer layer with a thickness of 15 nm and band gap of 3.2 eV is proposed. It is also shown that it is important to control the doping density of this layer in order to obtain a compromise between the p-n junction electric field and the global recombination rate, to produce efficient solar cells. After optimizing the studied solar cell, promising results are achieved with a conversion efficiency of 17.93%, a fill factor of 71.23%, a short-circuit current density of 30.92 mA/cm², and an open circuit voltage of 0.814 V. The obtained results will provide some important guidelines for producing high-efficiency $\text{Cu}_2\text{ZnSnS}_4$ solar cells.

topics: solar cell, CZTS, CdS, optimization

1. Introduction

The renewable energy sector continues to make remarkable progress, in particular photovoltaic (PV) technology. Today, the market for solar cells is still dominated by crystalline silicon despite different locks. The high cost of this type of cell is mainly due to the high use of the material and the expensive and complicated manufacturing processes [1, 2]. To get low-cost, high-efficiency solar cells, researchers turned to making thin film solar cells to use less material. However, the problem with this technology is that the first thin film solar cells, such as CdTe and CIGS, are made of rare and toxic elements [3].

In recent years, $\text{Cu}_2\text{ZnSnS}_4$ (CZTS), $\text{Cu}_2\text{ZnSnSe}_4$ (CZTSe), and $\text{Cu}_2\text{ZnSn}(\text{S},\text{Se})_4$ (CZTSSe) have emerged as replacement materials for thin film PV due to promising optoelectronic properties and the use of non-toxic, earth-abundant elements [4]. The CZTS was first studied as a solar cell material in 1988 at Shinshu University in

Japan [5]. It can be fabricated using different processes such as sputtering, evaporation, spray pyrolysis, electrodeposition, sol-gel technique, etc. [6]. Thin films based on CZTS show excellent photovoltaic properties such as direct band gap energy of 1.4–1.6 eV and absorption coefficient over 10⁴ cm⁻¹ [7]. In 2014, Wei Wang et al. [8] presented a record cell efficiency of around 12.6% using a hydrazine pure solution approach for a $\text{Cu}_2\text{ZnSnS}_4$ -based solar cell with 25 nm CdS buffer layer thickness [8, 9].

The main objective of this work is to reach a high-efficiency $\text{ZnO}/\text{CdS}/\text{CZTS}/\text{MoS}_2$ solar cell by optimizing the CdS buffer layer, using the SCAPS-1D simulator, through the analysis of the solar cell parameters variation, i.e., open-circuit voltage (V_{OC}), short-circuit current density (J_{SC}), fill factor (FF), and energy conversion efficiency (η), and also by understanding how the electric field, the recombination rate, and the quantum efficiency are affected by the buffer layer parameters.

2. Methodology and device structure

Numerical simulation is an essential tool to understand the mechanisms that govern the physics of the device and to test the viability of the proposed cell structure, as well as to predict the performance of solar cells before their elaboration. Solar Cell Capacitance Simulator (SCAPS-1D) is a one-dimensional solar cell simulation program developed at the Department of Electronic and Information Systems (ELIS) of the University of Gent, Belgium, and it is based on solving one-dimensional semiconductor basic equations (Poisson's equation and continuity equations of electrons and holes) [10–13].

The electrical, geometrical, and optical parameters of the simulated materials [14–18] are summarized in Table I.

All the simulations are conducted under standard solar illumination AM 1.5 at 1000 W/m² and a temperature of 25°C.

The schematic structure of the studied solar cell ZnO/CZTS/CdS /MoS₂ is shown in Fig. 1, where MoS₂ plays the role of the back surface field (BSF), CZTS — the absorber, CdS — the buffer layer, and ZnO — the window layer.

3. Results and discussion

The aim of this work is to optimize the CdS buffer layer by varying different controllable parameters within the experimental ranges. For this purpose we have studied the influence of doping density, thickness, and gap energy. The initial parameters of the CdS layer have been set at doping density $N_D = 5 \times 10^{18} \text{ cm}^{-3}$, thickness $W = 50 \text{ nm}$, gap energy $E_g = 2.4 \text{ eV}$.

3.1. Effect of the CdS buffer layer doping concentration

The effect of CdS buffer doping concentration on cell performance has been studied by varying the donor density of CdS from $N_D = 5 \times 10^{14} \text{ cm}^{-3}$ to $N_D = 5 \times 10^{21} \text{ cm}^{-3}$, while the other parameters have been kept constant. Figure 2 shows the effect of this variation on J_{SC} , V_{OC} , FF, and η .

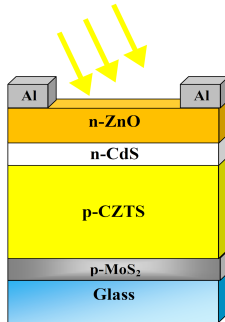


Fig. 1. Device structure of the studied solar cell.

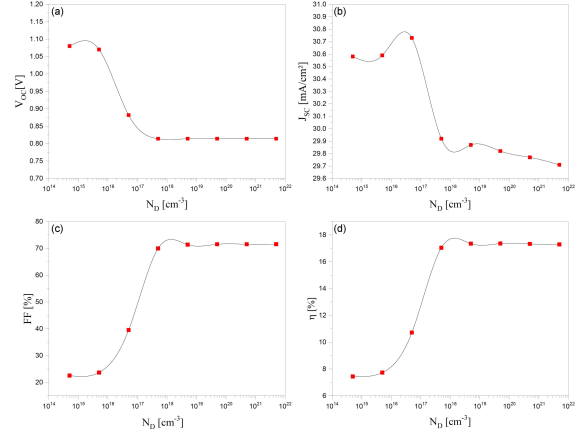


Fig. 2. Effect of the CdS buffer layer doping concentration N_D on (a) V_{OC} , (b) J_{SC} , (c) FF, and (d) efficiency η .

TABLE I

Simulation parameters for studied solar cell [14–18] Here, W [μm] is thickness, E_g [eV] is gap energy, χ [eV] is electron affinity, ϵ_r is dielectric permittivity, N_C [cm^{-3}] is effective conduction band density, N_V [cm^{-3}] is effective valence band density, μ_e [cm^2/Vs] is electron mobility, μ_p [cm^2/Vs] is hole mobility, N_D [cm^{-3}] is doping concentration of donors, N_A [cm^{-3}] is doping concentration of acceptors and N_t [cm^{-3}] is defect density.

Parameters	CZTS	CdS	ZnO	MoS ₂
W [μm]	1.1	0.015–0.18	0.08	0.1
E_g [eV]	1.4	2.3–3.2	3.3	1.7
χ [eV]	4.5	4.1	4.6	4.2
ϵ_r	10	10	9	13.6
N_C [cm^{-3}]	2.2×10^{18}	1.8×10^{19}	2.2×10^{18}	2.2×10^{18}
N_V [cm^{-3}]	1.8×10^{19}	2.4×10^{18}	1.8×10^{19}	1.8×10^{19}
μ_e [cm^2/Vs]	100	100	100	100
μ_h [cm^2/Vs]	25	25	25	25
N_D [cm^{-3}]	0	5×10^{14} – 5×10^{21}	1×10^{18}	0
N_A [cm^{-3}]	1×10^{16}	0	0	1×10^{16}
N_t [cm^{-3}]	5×10^{14}	1×10^{17}	1×10^{17}	1×10^{14}

The increase of the donor density greatly enhances the power efficiency of the cell (Fig. 2). Although the recombination rate becomes important in the buffer layer with the carriers density increase, as can be seen in Fig. 3, the recombination rate decreases in the active layer, which improves the conversion efficiency that goes from 7.44% to more than 17% when the doping density increases from 5×10^{14} to $5 \times 10^{18} \text{ cm}^{-3}$.

On the other hand, the efficiency increases gradually until the doping density reaches $5 \times 10^{18} \text{ cm}^{-3}$ because a strong doping density increases the electric field on the CZTS/CdS junction and the CdS/ZnO junction (Fig. 4), which will promote the separation of the photo-generated charges. However, as can be seen in Fig. 2, the efficiency stabilizes

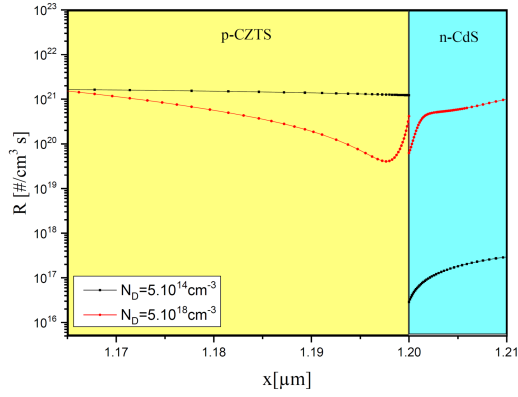


Fig. 3. Influence of the CdS doping density on the recombination rate.

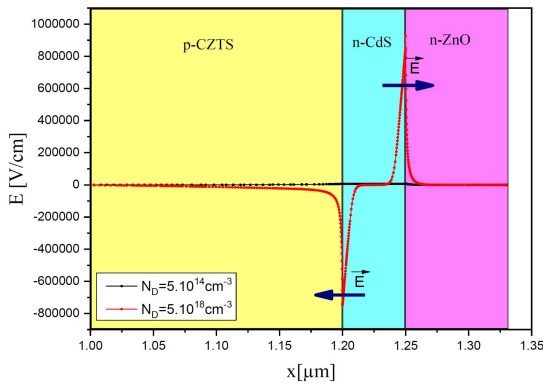


Fig. 4. Influence of the CdS doping density on the electric field at the junctions CZTS/CdS and CdS/ZnO.

from a charge density of $5 \times 10^{18} \text{ cm}^{-3}$ because the recombination process will be amplified, and the probability of collecting the photo-generated carriers will decrease.

In the heavily doped buffer layer, large traps for charge carriers are generated, and the probability of interaction is increased [19]. As the lifetime of charge carriers is inversely proportional to the trap concentration [16, 20], the recombination rate increases and therefore J_{SC} sharply decreases after $N_D = 1 \times 10^{17} \text{ cm}^{-3}$.

3.2. Effect of the CdS buffer layer thickness

The effect of the CdS buffer layer thickness on the performance of $\text{MoS}_2/\text{CZTS}/\text{CdS}/\text{ZnO}$ solar cell has been studied by varying it from 15 to 180 nm, while the doping density of the same layer has been set to the optimum value found previously. We have shown in Fig. 5 the different effects of this variation on the photovoltaic parameters of the cell.

As shown in Fig. 5, V_{OC} is not affected by the buffer layer thickness. Its value remains around 814 mV, while the FF increases slightly and J_{SC} decreases from 30.68 to 27.63 mA/cm^2 when the thickness increases from 15 to 180 nm, generating a large decrease in efficiency, which goes from 17.80%

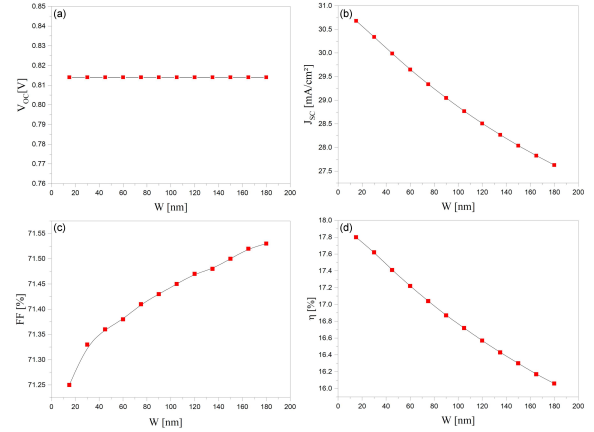


Fig. 5. Effect of the buffer thickness variation on (a) V_{OC} , (b) J_{SC} , (c) FF, (d) efficiency η .

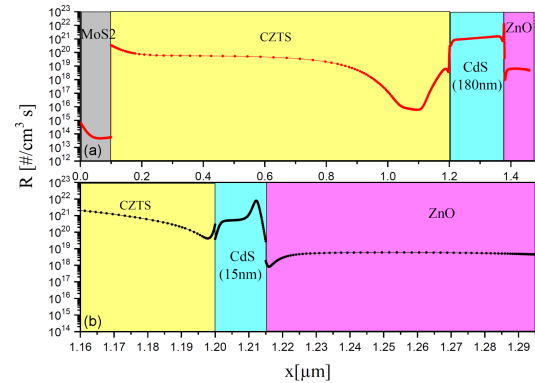


Fig. 6. Influence of the CdS buffer layer thickness on the recombination rate for two thicknesses of the CdS layer: (a) $W = 180 \text{ nm}$, (b) $W = 15 \text{ nm}$.

to 16.06%. This diminution is due to the fact that when the thickness of the buffer layer increases, the photo-generated carriers must cross longer distances than their diffusion lengths, and will be recombined before being collected, which increases the recombination rate that has been represented in Fig. 6.

Figure 7 shows the variation of the cell's quantum efficiency for two values of the buffer layer thickness. When the latter increases, more incident photons will be absorbed into the buffer layer, and fewer photons will be captured in the absorber layer [21]. Therefore, the photons absorbed in the CZTS layer would make fewer electron-hole pairs and cause a reduction in current and efficiency [22].

The quantum efficiency for a small CdS thickness is clearly better for wavelengths between 300 and 550 nm because short wavelength photons generate electron-hole pairs, which could be collected since their diffusion lengths are enough to reach the contacts before recombining. The optimal value of buffer layer thickness is taken equal to 15 nm. This drastic reduction of the CdS layer allows to reduce the production cost of the cell and the quantity of toxic material used.

3.3. Effect of the CdS buffer layer gap energy

In Fig. 8, we present the impact of different gap energies of the CdS buffer layer on the cell's outputs — the gap energy was changed from 2.3 to 3.2 eV.

With the increase of the buffer layer band gap, no major change in V_{OC} and FF is observed. However, an improvement in J_{SC} and hence in efficiency is observed. As we can see in Fig. 9, with the increase of the band gap of CdS, the recombination rate decreases in the emitter layer. Indeed, for a wide CdS band gap, low energy photons will not be absorbed in the CdS buffer layer but will be able to pass into the active layer, where they will be absorbed thanks to the low gap of the CZTS (1.4 eV), and this will increase the photo-generated charge carriers and thus will generate a high short-circuit current density.

In order to confirm this, we have plotted in Fig. 10 the quantum efficiency for two different values of the band gap. We can conclude that the best efficiency is obtained for $E_g = 3.2$ eV. Therefore, it is important to choose a buffer layer with a wide band gap to obtain the best solar cell performance.

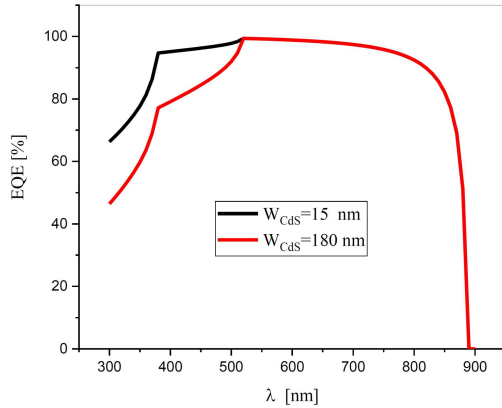


Fig. 7. The quantum efficiency curves versus wavelength for different thicknesses of buffer layer.

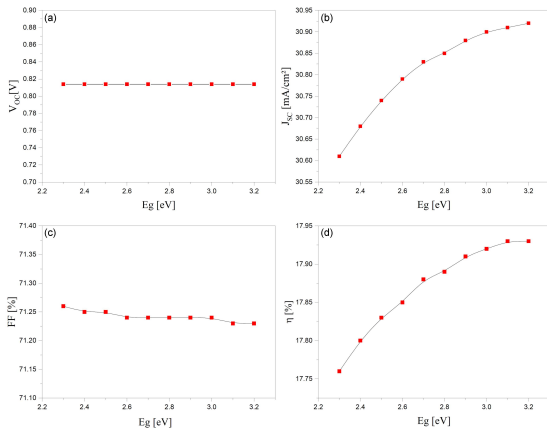


Fig. 8. Effect of the CdS buffer gap energy on: (a) V_{OC} , (b) J_{SC} , (c) FF, (d) efficiency.

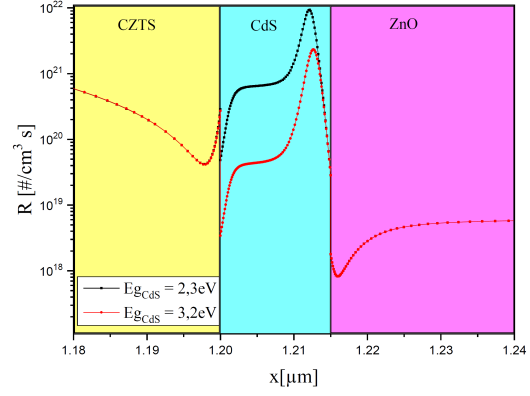


Fig. 9. Influence of the CdS buffer layer band gap on the recombination rate.

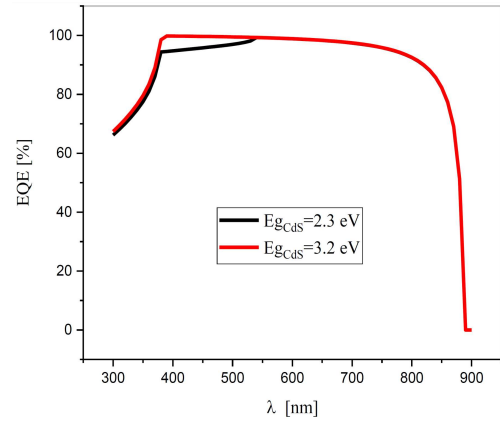


Fig. 10. The quantum efficiency curves versus wavelength for two different buffer layer band gaps.

The optimal CdS gap energy was set at 3.2 eV, which is compatible with thin layers characterized by wide gaps. Moreover, the formation of alloys (CdS:O) is an effective way to increase the CdS optical bandgap. By controlling the ratio of O_2/Ar in the sputtering ambient, the band gap of CdS:O can be tuned from 2.4 to 3.8 eV [18, 23–25].

4. Conclusion

In this work, theoretical simulations were performed to find the optimal parameters of CdS buffer layer. In addition to the current density–voltage characteristics ($J(V)$) study, we also tried to explain the physical phenomena, which induce the obtained results by studying the electric field, the recombination rate, and the quantum efficiency of the cell. The obtained results indicate that the increase of the CdS buffer layer thickness deteriorates the cell's performance because the diffusion length of the carriers becomes too small compared to the distances to cross. The doping density of the CdS buffer layer plays an important role in improving cell efficiency. It has been shown that it is important to find a compromise in the doping density, as an increase in doping density causes two opposite effects: an increase

in the electric field, which influences positively the efficiency, and an increase in the recombination rate, which influences negatively the efficiency.

This study allowed us to optimize the solar cell having the structure ZnO/CdS/CZTS/MoS₂ and to obtain an efficiency of 17.93%. The best performances are obtained for a low CdS layer thickness of only 15 nm, which is advantageous, thanks to the reduction in the quantity of cadmium used for the buffer layer elaboration. The optimal CdS gap energy was set at 3.2 eV. This large gap value can be obtained by doping the CdS with oxygen [18, 23–25].

These findings are very promising and can provide helpful guidance for experimentalists in the manufacture of high-performance CZTS solar cells.

Acknowledgments

The authors would like to acknowledge Dr. Marc Burgelman from the University of Gent, Belgium, for providing the SCAPS-1D simulator.

References

- [1] M. Okil, M.S. Salem, T.M. Abdolkader, A. Shaker, *Silicon*, 1 (2021).
- [2] J. Yu, J. Li, Y. Zhao, A. Lambertz, T. Chen, W. Duan, W. Liu, X. Yang, Y. Huang, K. Ding, *Solar Energy Mater. Solar Cells* **224**, 110993 (2021).
- [3] M. Jamil, M. Amami, A. Ali, K. Mahmood, N. Amine, *Solar Energy* **231**, 41 (2022).
- [4] F. Belarbi, W.L. Rahal, D. Rached, S. Benghabrit, M. Adnane, *Optik* **216**, 164743 (2020).
- [5] T. K. Ito Nakazawa, *Jpn. J. Appl. Phys.* **27**, 2094 (1988).
- [6] A. Tombak, T. Kilicoglu, Y.S. Ocak, *Renew. Energy* **146**, 1465 (2020).
- [7] P. Kuch, K. deori, A. Kumar, S. Deka, *J. Mater. Chem. A* **3**, 8098 (2015).
- [8] W. Wang, M.T. Winkler, O. Gunawan, T. Gokmen, T.K. Todorov, Y. Zhu, D.B. Mitzi, *Adv. Energy Mater.* **4**, 1301465 (2014).
- [9] L. Sravani, S. Routray, Maykel Courel, K.P. Pradhan, *Solar Energy* **227**, 56 (2021).
- [10] M. Burgelman, J. Verschraegen, S. Degrave, P. Nollet, *Prog. Photovolt. Res. Appl.* **12**, 143 (2004).
- [11] J. Verschraegen, M. Burgelman, *Thin Solid Films* **515**, 6276 (2007).
- [12] K. De cock, S. Khelifi, M. Burgelman, *Thin Solid Films* **519**, 7481 (2011).
- [13] S. Noor Alhuda, T. Al-Jammas, Q. Algwari, *Solid State Technology* **63**, 1703 (2020).
- [14] Y.H. Khattak, F. Baig, S. Ullah, B. Marí, S. Beg, H. Ullah, *J. Renew. Sustain. Energy* **10**, 033501 (2018).
- [15] F.A. Jhuma, M.Z. Shaily, M.J. Rashid, *Mater. Renew. Sustain. Energy* **8**, (2019).
- [16] A. Luque, S. Hegedus, *Handbook of Photovoltaic Science and Engineering*, John Wiley & Sons, Chichester 2010.
- [17] A.I. Oliva, O. Solís-Canto, R. Castro-Rodríguez, P. Quintana, *Thin Solid Films* **391**, 28 (2001).
- [18] C. Ou, K. Shen, Z. Li, H. Zhu, T. Huang, Y. Mai, *Solar Energy Mater. Solar Cells* **194**, 47 (2019).
- [19] A.E.H. Benzetta, M. Abderrezek, M.E. Djeghlal, *Optik* **204**, 164155 (2020).
- [20] H. Zhou, J. Yu, H. Jia, H. Zhang, S. Cheng, *Micro Nano Lett.* **11**, 386 (2016).
- [21] O.K. Simya, A. Mahaboobatcha, K. Balachander, *Superlattices Microstruct.* **82**, 248 (2015).
- [22] S. Enayati Maklavani, S. Mohammadnejad, *Opt. Quant. Electron.* **2**, 22 (2020).
- [23] D.M. Meysing, C.A. Wolden, M.M. Griffith, H. Mahabuduge, J. Pankow, M.O. Reese, J.M. Burst, W.L. Rance, T.M. Barnes, *J. Vac. Sci. Technol. A* **33**, 021203 (2015).
- [24] D.M. Meysing, M.O. Reese, C.W. Warren et al., *Solar Energy Mater. Solar Cells* **157**, 276 (2016).
- [25] J. Ge, P. Koirala, C.R. Grice, P.J. Roland, Y. Yu, X. Tan, R.J. Ellingson, R.W. Collins, Y. Yan, *Adv. Energy Mater.* **7**, 1601803 (2017).